Published in final edited form as:
J Comp Neurol. 2014 December 1; 522(17): 3834–3846. doi:10.1002/cne.23643.

The orexinergic neurons receive synaptic input from C1 cells in rats

Genrieta Bochorishvili, **Thanh Nguyen**, **Melissa B. Coates**, **Kenneth E. Viar**, **Ruth L. Stornetta**, and **Patrice G. Guyenet**
Department of Pharmacology, University of Virginia, Charlottesville, VA

Abstract

The C1 cells, located in the rostral ventrolateral medulla (RVLM), are activated by pain, hypoxia, hypoglycemia, infection and hypotension and elicit cardiorespiratory stimulation, adrenaline and ACTH release, and arousal. The orexin neurons contribute to the autonomic responses to acute psychological stress. Here, using an anatomical approach, we consider whether the orexin neurons could also be contributing to the autonomic effects elicited by C1 neuron activation.

Phenylethanolamine N-methyl transferase-immunoreactive (PNMT-ir) axons were detected amongst orexin-ir somata and close appositions between PNMT-ir axonal varicosities and orexin-ir profiles were observed. The existence of synapses between PNMT-ir boutons labeled with diaminobenzidine and orexinergic neurons labeled with immunogold was confirmed by electron microscopy. We labeled RVLM neurons with a lentiviral vector that expresses the fusion protein ChR2-mCherry under the control of the catecholaminergic neuron-selective promoter PRSx8 and obtained light and ultrastructural evidence that these neurons innervate the orexin cells. Using a Cre-dependent adeno-associated vector and TH-Cre rats we confirmed that the projection from RVLM catecholaminergic neurons to the orexinergic neurons originates predominantly from PNMT-ir catecholaminergic (i.e. C1 cells). The C1 neurons were found to establish predominantly asymmetric synapses with orexin-ir cell bodies or dendrites. These synapses were packed with small clear vesicles and also contained dense core vesicles.

In summary, the orexin neurons are among the hypothalamic neurons contacted and presumably excited by the C1 cells. The C1-orexin neuronal connection is probably one of several suprabulbar pathways through which the C1 neurons activate breathing and the circulation, raise blood glucose and facilitate arousal from sleep.

Address correspondence to: Patrice G. Guyenet, PhD, University of Virginia Health System, P.O. Box 800735, 1300 Jefferson Park Avenue, Charlottesville, VA 22908-0735. Tel: (434) 924-7433; Fax: (434) 982-3878; pgg@virginia.edu.

CONFLICT OF INTEREST STATEMENT
The authors declare that there are no conflicts of interest.

ROLE OF AUTHORS
All authors had full access to all the data in the study and take responsibility for the integrity of the data and the accuracy of the data analysis. Study concept and design: GB, RLS, PGG Acquisition of data: GB, TN, MBC, KEV, RLS. Analysis and interpretation of data: GB, TN, RLS, PGG. Drafting of the manuscript: RLS, PGG.

INTRODUCTION

The C1 neurons reside in the rostral ventrolateral medulla (RVLM) (for review {Guyenet, 2013 15248/id}). Originally defined by their ability to synthesize catecholamines (indicated by tyrosine hydroxylase (TH) immunoreactivity) including adrenaline (indicated by phenylethanolamine-N-methyl transferase (PNMT) immunoreactivity), these cells signal via multiple additional transmitters, notably glutamate and peptides (NPY, enkephalin, substance P and others) (Farnham et al., 2008; Stornetta, 2009; Depuy et al., 2013; Abbott et al., 2014). Arterial pressure regulation and CRF/ACTH release were the first well-documented functions of the C1 neurons (Reis et al., 1989; Ericsson et al., 1994; Ruggiero et al., 1994). Blood pressure control was attributed to their direct projections to the intermediolateral cell column whereas ACTH release was considered to rely on their input to the paraventricular nucleus of the hypothalamus (Hokfelt et al., 1974; Ross et al., 1981; Ericsson et al., 1994; Card et al., 2006; Abbott et al., 2013b). However, the C1 cells also regulate blood glucose and the parasympathetic outflow, stimulate breathing and sighing, activate the locus coeruleus and probably produce arousal from sleep (Li et al., 2009; Ritter et al., 2011; Depuy et al., 2013; Abbott et al., 2013b). In sum, the C1 neurons seem to respond to a wide variety of stimuli (e.g. pain, hypotension, hypoxia, infection) and have the potential to contribute to the stereotyped pattern of cardiovascular, respiratory and endocrine responses typically associated with acute stress (Guyenet et al., 2013).

The C1 cells project to the region of the hypothalamus that contains the orexinergic neurons (Card et al., 2006; Abbott et al., 2013b). The latter neurons discharge in a state-dependent manner with maximal activity during waking and lowest activity during REM sleep (Estabrooke et al., 2001; Lee et al., 2005). The absence of orexin (a.k.a hypocretin) causes narcolepsy, a state of irregular transition from REM sleep to normal sleep (Scammell et al., 2001). Conversely, direct stimulation of orexin neurons facilitates the transition from slow wave sleep or REM sleep to wakefulness (Adamantidis et al., 2007). Consistent with their pattern of activity and their projections to the spinal cord and the lower brainstem, the orexinergic neurons contribute to maintaining a higher blood pressure and breathing intensity selectively during the waking state (Peyron et al., 1998; Kuwaki et al., 2008; Kuwaki, 2010). The orexin neurons also contribute to the increased sympathetic tone and blood pressure of spontaneously hypertensive rats (Li et al., 2013a). Although work done in anesthetized or reduced preparations suggests that the C1 cells activate blood pressure via direct projections to sympathetic preganglionic nerves, the preceding considerations suggest that, in conscious animals, the C1 cells could also be activating arterial pressure via more circuitous routes involving the hypothalamus. The present ultrastructural study is designed to explore the possibility that the C1 cells of the rat are in a position to regulate the activity of the orexinergic neurons.

MATERIALS AND METHODS

Animals

Adult male Sprague-Dawley rats (Taconic) or TH-Cre rats on a Long Evans background (Witten et al., 2011) procured from I. Witten (Princeton University, Princeton, NJ) and K. Deisseroth (Stanford University, Stanford, CA)) were used for all experiments. Animals

were housed in pairs and received food and water ad lib. The Institutional Animal Care and Use Committee at the University of Virginia approved all protocols.

Surgery

Four male Sprague Dawley rats (225–250 g; Taconic, Germantown, NY) and 3 male TH-Cre rats (225–250 g, were anesthetized with an intramuscular bolus of ketamine (75 $mg \cdot kg^{-1}$), xylazine (5 $mg \cdot kg^{-1}$) and acepromazine (1 $mg \cdot kg^{-1}$) with supplemental doses (10% of original dose) delivered as needed to prevent the corneal reflex and withdrawal of a hind limb in response to a firm paw pinch. The Sprague Dawley rats received injections of a lentiviral vector encoding channel channelrhodopsin-2 (ChR2, H134R) fused to mCherry under the control of PRSx8 (PRSx8-ChR2-mCherry)(Hwang et al., 2001; Abbott et al., 2009a). This vector has been shown to label catecholamine neurons throughout their axons and terminals {Abbott, 2012 14830/id}. A total volume of 600 nL was injected unilaterally into RVLM using previously described methods (Abbott et al., 2012) (approximate stereotaxic coordinates: 1.9 mm lateral, 2.7–3.1 mm caudal to lambda and 8.5–9.0 mm ventral from the surface of the brain). Three TH-Cre rats were treated in an identical manner with the exception that a cre-dependent AAV (serotype 2) encoding eYFP under the control of the EF1alpha promoter (DIO-EF1α-eYFP AAV2) was injected in place of the PRSX8-ChR2-mCherry lentivirus. The lentiviral vector was produced and tittered at the University of North Carolina Vector Core (Chapel Hill, NC) from a previously described plasmid (Abbott et al., 2009a). The DIO-EF1a-eYFP AAV2 was obtained as a stock aliquot from the UNC vector core.

Perfusions

Light Microscopy—After 4–6 weeks, the TH-Cre The DIO-EF1a-eYFP AAV2 –injected rats and 3 male Sprague-Dawley naïve rats (225–250 g) (controls) were anesthetized with pentobarbital i.p. (65 mg/kg) and perfused transcardially first with a phosphate buffered saline rinse and then with 4% paraformaldehyde. Brains were removed and post fixed for up to 48 hours in 4% paraformaldehyde at 4 C.

Electron Microscopy—After 4–6 weeks, the 4 PRSX8-ChR2-mCherry-injected Sprague-Dawley rats and 3 male Sprague-Dawley naïve rats (225–250 g) (controls) were anesthetized as described above and perfused transcardially first with heparinized saline followed by 2% paraformaldehyde with 3.75% acrolein (Electron Microscope Sciences), followed by 2% paraformaldehyde. The brains were removed and postfixed from 4–24 hours in 2% paraformaldehyde.

Histology

Coronal sections of brainstem (30 mm) and forebrain (45 mm) were made on a vibrating microtome and stored in cryoprotectant at −20° C awaiting further processing.

Light microscopy—All procedures were done on free-floating sections with a Tris-buffered saline diluent. For verification of the injection site, a 1 in 6 series of coronal sections was processed with antibodies for detection of mCherry (rabbit anti-dsRed, 1:500; Clontech) or eYFP (chicken anti-GFP, 1:1,000; Aves Labs), tyrosine hydroxylase (TH)

(sheep anti-TH, 1:2000; Millipore) or phenyl-ethanolamine-N-methyl transferase (PNMT) (rabbit-anti-PNMT, 1:10,000; M. Bohn, Northwestern University). Sections were first rinsed, blocked in 10% horse serum with 0.1% Triton, then placed in primary antibodies. After overnight incubation in primary antibodies, sections were rinsed and incubated in secondary antibodies (all made in donkey against the respective species of the primary antibodies (1:200; Jackson ImmunoResearch) and tagged with: for dsRed, Cy3; for TH, Alexa 488; for PNMT, Cy3; for eYFP, Alexa 488.

Forebrain sections were processed with antibodies for detection of orexin (goat anti-orexin, 1:5,000; Santa Cruz Biotechnology), mCherry (rabbit anti-dsRed, 1:500; Clontech) or eYFP (chicken anti-GFP, 1:1,000; Aves Labs) and TH (sheep anti-TH, 1:2000; Millipore) or PNMT (rabbit-anti-PNMT, 1:10,000; M. Bohn, Northwestern University). After overnight incubation in primary antibodies, sections were rinsed and incubated in secondary antibodies (all made in donkey against the respective species of the primary antibodies (1:200; Jackson ImmunoResearch) and tagged with: for orexin, Cy3 or DyLight 649; for TH, Alexa 488; for PNMT, Dylight 649; for eYFP, Alexa 488.

After 45–60 minute incubation in secondaries, sections were rinsed, mounted onto gel coated slides, air dried, dehydrated through alcohols and xylenes and coverslips affixed with DPX mountant.

Electron microscopy—Sections for electron microscopy were treated with 1% sodium borohydride (Sigma-Aldrich), then rinsed, blocked in 10% horse serum with 0.04% Triton x 100 and incubated in primary antibodies for detection of mCherry as described above. After overnight incubation in primary antibodies, sections were incubated for 60 min in biotinylated donkey anti-rabbit IgG (1:400, Jackson ImmunoResearch), rinsed and incubated for another 60 min in avidin-biotin peroxidase complex (ABC Vectastain Elite at 1:100; Vector Labs). The sections were treated with 3–3′ diaminobenzidine (DAB) using a DAB kit according to manufacturer's instructions (Vector Labs) and 0.003% hydrogen peroxide (Sigma Aldrich) for 6 minutes. After this point, sections were incubated in goat anti-orexin (1:5000; Santa Cruz) at 4° C overnight. Sections were rinsed and incubated for 30 minutes in a washing buffer made of PBS containing 1% BSA, 0.1% fish gelatin. The tissue was then incubated for two hours with 1 nm gold-donkey anti-goat IgG (1:50; Aurion, Electron Microscopy Sciences, Hatfield, PA). The sections were next rinsed and incubated in 2.5% glutaraldehyde in PBS for 10 minutes. The sections were transferred to sterile, untreated culture well plates for a series of rinses followed by silver enhancement reaction at room temperature in IntenSEM silver kit reagents (GE Healthcare, Chalfont St. Giles, UK). Sections were rinsed and incubated in 0.5–1% osmium tetroxide (Electron Microscopy Sciences) for 60 min, rinsed and incubated for 90 min in 1% of uranyl acetate (Electron Microscope sciences). The tissue was rinsed dehydrated through increasing ethanol concentrations then treated with propylene oxide and incubated in a 1:1 mixture of propylene oxide and embedding resin Embed-812 (Electron Microscopy Sciences). This mixture was then replaced with 100% Embed-812 and allowed to infiltrate the sections for 10–12 hours. The tissue was embedded between sheets of plastic, flattened and cured for at least 72 hours at 62° C.

Microscopic examination, mapping and photography

Light microscopy—Sections were examined with a wide field fluorescent microscope (Zeiss AxioIamger) and cells or terminals mapped with a computer-assisted mapping program (Neurolucida, v 10; MicroBrightField, Williston, VT; RRID:nif-0000-10294) as previously described (Bochorishvili et al., 2012; Abbott et al., 2013b). Images were digitally captured with a Zeiss Mrc camera (1388×1040 resolution) and the resulting TIFF files were imported into the Canvas drawing software (v. 10, ACDC, Miami, FL). Output levels were adjusted to include all information-containing pixels. Balance and contrast was adjusted to reflect true rendering as much as possible. No other photo-retouching was done. Figures were assembled and labeled within the Canvas software. Z-stacks were constructed using the computer interface-motor-driven stage by capturing images using different filter sets at 0.3 micron z intervals through tissue depths of 5–10 microns. The resulting images were subjected to 3D blind deconvolution through 10 iterations using the AutoQuant X3 software (Media Cybernetics, Rockville, MD; RRID:SciRes_000125). Deconvoluted stacks were then processed with Volocity 3D image Analysis software (version 4.4, Improvision; RRID:SciRes_000112) for 3D rendering and confirmation of close appositions as detailed in (Holloway et al., 2013).

Electron microscopy—Flat-embedded sections were examined with a the Zeiss AxioImager light microscope to detect immunogold-labeled orexin-cells and DAB -labeled C1 terminal fields in the forebrain. The regions of interest were further trimmed and repolymerized at the bottom of BEEM capsules. The resulting block was trimmed to a 2 X 1 mm trapezoidal block that contained the orexin-labeled cells. Ultrathin sections (70–90 nm) were cut (Leica Ultracut UCT) and collected onto copper mesh grids in series of seven to ten sections per grid and 20–30 sections for serial analysis. Tissue was analyzed by using an JEOL 1230 transmission electron microscope (Peabody, MA), and micrographs were captured by using ultra high resolution digital imaging CCD camera from Advanced Microscopy Facility (Charlottesville, VA). Adobe Photoshop was used to adjust image contrast and illumination, and then images were exported into the Canvas drawing software.

Antibodies

All antibodies used are listed in the Journal of Comparative Neurology antibody database and are described in Table 1.

1. The orexin antibody was a goat polyclonal antibody (Santa Cruz Biotechnology, Santa Cruz, CA; catalog No. SC-8070, C-19; RRID:AB_2315772) raised against a peptide mapping at the carboxy terminus of human orexin A (residues 48–66 of the orexin precursor, identical to the corresponding mouse sequence; manufacturer's technical information). The specificity of this antibody has previously been verified by preabsorption with orexin, which abolished all staining and by Western blots of mouse brain extract which shows a single band at the expected molecular weight (manufacturer's technical information).
2. Rabbit anti-DsRed polyclonal antibody (Living Colors DsRed polyclonal antibody 632496; Clontech, Mountain View, CA; RRID:AB_10015246) was raised against DsRed-Express, a variant of Dicosoma sp. red fluorescent protein. It recognizes all

the red fluorescent “fruit” protein variants including mCherry. According to the manufacturer, a specific band of 30–38 kDa was observed on Western blots of lysates of HEK 293 cells expressing DsRed-express or DsRed- monomer. In the current study, no labeling was present in tissue without injections of the ChR2-mCherry lentivirus.

3. PNMT antibody raised in rabbits against purified rat adrenal extract was obtained from M. Bohn (Northwestern University, Chicago, IL; Bohn et al., 1987; RRID:AB_2315181) and matched labeling described previously published by our laboratory (Verberne et al., 1999) and others (Ruggiero et al., 1994).

4. TH mouse anti-sheep antibody (AB1542; Millipore, Billerica, MA; RRID:AB_90755) was raised against native tyrosine hydroxylase from rat pheochromocytoma. As reported by Millipore, this antibody recognizes a protein of approximately 60 kDa by Western blot of mouse brain lysate. The labeling produced in the current study was seen in cell soma and dendrites as well as putative terminals, and the pattern of labeling was restricted to known catecholamine cell groups. The immunolabeling with TH observed in the present study was similar to that seen in many previous studies in our laboratory using similar methods (Kang et al., 2007; Takakura et al., 2008; Abbott et al., 2009b).

5. GFP antibody raised in chicken against recombinant GFP protein (RRID:AB_1000024; Aves Labs, Tigard, OR) shows labeling only in tissue injected with viral vectors expressing eYFP. The antibody labeling matches exactly with non-amplified eYFP fluorescence.

RESULTS

PNMT-containing terminals make synapses with the orexinergic neurons

A moderately dense plexus of PNMT-immunoreactive (ir) axons was present in the hypothalamic region that contains orexin-ir somata (Bregma level −2.80 mm and −3.60 mm). Higher densities were present in the dorsomedial and paraventricular nuclei (not illustrated). Close appositions between PNMT-ir axonal varicosities and orexin-ir profiles were commonly observed (Fig. 1). Further examination of such close appositions processed with Volocity 3D Image Analysis software (PerkinElmer, Waltham, MA) suggested that some of these appositions might be synaptic contacts (Fig. 1B,C).

We did an ultrastructural study in three rats to confirm the existence of synapses between PNMT-ir boutons labeled with DAB and orexinergic neurons labeled with immunogold. PNMT immunoreactivity was identified in axon terminals (Fig. 2A–D) and unmyelinated axons. PNMT-ir axon terminals contained dense-core vesicles (white arrows in Fig. 2A–D) and, without exception, an abundance of small clear synaptic vesicles (Fig. 2A–D). PNMT-ir terminals made synaptic contacts mostly with small and medium-sized dendrites (Fig. 2A–D) and less frequently with neuronal cell bodies. We focused our attention on the synapses between PNMT-ir terminals and putative orexinergic profiles (immunogold positive). Asymmetric synapses, characterized by thick, electron-dense postsynaptic densities (Gray’s type I) predominated over symmetric densities (Gray’s Type II) (Fig. 2A–C; 73 vs. 19).

Most of these synapses were observed on dendrites as opposed to cell bodies (67 vs. 6). Symmetric synapses were also observed predominantly on dendrites rather than cell bodies (17 vs. 2). Within the region of interest, the majority of PNMT-ir terminals that made recognizable synapses (77%) contacted orexin-ir profiles.

The C1 neurons contribute to the adrenergic innervation of the orexin cells

The C1 neurons are the largest but not the only cluster of PNMT-ir neurons in the brain of rats (Minson et al., 1990). The next experiments were designed to ascertain that the orexin neurons receive input specifically from the C1 cells. To address this question, we first obtained light microscopic evidence that the C1 cells might innervate the orexinergic neurons and then we performed ultrastructural studies to confirm this interpretation.

For light microscopy and ultrastructural studies we labeled RVLM neurons with a lentiviral vector that expresses the fusion protein ChR2-mCherry under the control of the catecholaminergic neuron-selective promoter PRSx8 (Hwang et al., 2001) (PRSX8-ChR2-mCherry). As shown previously (Abbott et al., 2009b), this method is highly, albeit not perfectly, selective for catecholaminergic neurons (Fig. 3A). In the 3 rats examined, most of the mCherry-ir neurons (respectively 93, 76, 75%; average 81%) were TH-ir. These neurons were confined to the RVLM between 11.8 and 12.8 mm caudal to bregma (Paxinos and Watson, 2005). In each brain, large numbers of mCherry-ir fibers and axonal varicosities were present within the orexin-rich region of the hypothalamus (Fig. 3C,D) and close appositions between these varicosities and orexin-ir profiles were frequently detected. However, because the antibodies available to detect mCherry and PNMT were both raised in rabbits, we could not test whether the mCherry-ir terminals located in the orexin-rich region actually contained PNMT. In order to test more directly that the C1 cells innervate the orexin-rich region of the hypothalamus, we performed an additional anterograde tracing experiment in three TH-Cre rats. The Cre-dependent viral vector DIO-Ef1α-ChR2-eYFP-AAV2 (DIO-AAV) (Cardin et al., 2010) was injected into the left RVLM of these rats which resulted in the highly selective expression of eYFP by PNMT-ir neurons (Fig. 3B). Specifically, 87, 86 and 73% (average 82%) of the eYFP-ir neurons were found to contain PNMT immunoreactivity. These neurons were confined to the ventrolateral medulla between 11.2 and 12.8 mm caudal to bregma (Paxinos and Watson, 2005). Visual inspection of the orexin-rich region of the hypothalamus showed that the vast majority of the eYFP-ir axonal varicosities were PNMT-positive (Fig. 3E–H).

Ultrastructural studies on the hypothalamus were carried out with tissue from the three adult rats injected with PRSX8-mCherry-ChR2 lentivirus. mCherry-ir terminals were found to establish typically asymmetric synapses with orexin-ir cell bodies or dendrites. Figure 4A,B shows two serial, albeit non-consecutive, sections through an mCherry-labeled asymmetric synapse with an orexin-ir dendrite (immunogold showing the presence of orexin in panel A, mCherry-labeled asymmetric synapse in panel B). Two additional examples of asymmetric synapses between a terminal immunoreactive for mCherry and an orexin-ir dendrite are shown in Figure 4C and D. In the hypothalamic region investigated most of the mCherry-ir axon terminals that made recognizable synapses established such asymmetric synapses with

orexin-ir neurons (72%, n=92). Most of these synapses were with orexin-ir dendrites (88 of 92) and the rest with cell bodies.

DISCUSSION

The present study reveals that the orexin neurons are among the hypothalamic neurons contacted and presumably excited by the C1 cells. The C1-orexin neuronal connection is likely to represent an indirect and state-dependent route through which the RVLM regulates breathing, the circulation and blood glucose. This connection could also partly explain why C1 cell stimulation produces arousal (Abbott et al., 2013a).

The C1 cells innervate the orexinergic neurons

In rats, PNMT-synthesizing neurons are confined to the medulla oblongata and consist of three clusters. The C1 group, located in the rostral ventrolateral medulla is the largest with 72% of the cells, the C2 and C3 clusters, located respectively in the rostral portion of the nucleus of the solitary tract and in the rostral part of the dorsomedial medulla contain 13% (C2) and 15% (C3) of the PNMT-ir neuron population in rats (Minson et al., 1990). Whether or not the C2 and C3 adrenergic neurons contribute to the PNMT innervation of the orexin neurons was not tested in the present work and remains a possibility. Based on our anterograde tracing with viral vectors, the C1 cell group clearly projects to the orexin-rich region of the hypothalamus. Consistent results were produced by two approaches, the first based on the use of a Cre-dependent AAV2 in TH-Cre rats and the other relying on the PRSx8-promoter in a lentiviral vector that was injected into Sprague-Dawley rats. The PRSx8 driven ChR2-mCherry lentivirus is largely but not totally catecholaminergic-specific. When injected into the RVLM, this vector also transduces retrotrapezoid nucleus (RTN) neurons and a few cholinergic neurons (Card et al., 2006; Abbott et al., 2009a). The relative proportion varies depending on the injection site and additional factors such as titer and time after vector injection. RTN neurons do not innervate the hypothalamus and could not have contributed to the RVLM innervation of the orexin neurons (Abbott et al., 2009a; Bochorishvili et al., 2012). PRSx8-driven lentiviral vectors also transduce a subset of cholinergic neurons, probably parasympathetic preganglionic neurons and nucleus ambiguus motor neurons (Duale et al., 2007; Abbott et al., 2009a). However, these cholinergic neurons, like RTN neurons, do not innervate the hypothalamus. In sum, both approaches used here labeled catecholaminergic axons very specifically within the hypothalamus and the experiments performed in the TH-Cre rats indicated that these catecholaminergic neurons were largely C1 cells because their hypothalamic axonal processes were predominantly PNMT-ir. Nonetheless, a small minority of noradrenergic neurons (A1 and or A5 neurons) could have also contributed to these projections because both vectors transduce noradrenergic neurons and a few noradrenergic neurons are co-mingled with the C1 cells, even in the most rostral aspect of the ventrolateral medulla.

The ultrastructural characteristics of the synapses made by the virally transduced C1 neurons onto orexin neurons were indistinguishable from those of previously examined C1 cell synapses (Milner et al., 1988; Milner et al., 1989; Depuy et al., 2013; Holloway et al., 2013). Of note, a large majority of them were asymmetric (Gray type I). The symmetric (Gray type

II) appearance of the remainder could be explained by the possibility that the plane of section only grazed the post-synaptic density. Like elsewhere in the brain, the synapses established by the C1 cells with the orexinergic cells were densely filled with small clear vesicles. These vesicles are likely to store glutamate since the C1 neurons, including those with hypothalamic projections, express VGLUT2 but lack markers of glycinergic or GABAergic transmission (i.e. GlyT2 or GAD1 mRNA or protein immunoreactivity) (Stornetta et al., 2002; Depuy et al., 2013; Guyenet et al., 2013; Holloway et al., 2013; Abbott et al., 2014).

Functional significance: the orexinergic neurons likely contribute to the cardiorespiratory and arousal effects of the C1 cells

The roughly one third of the C1 neurons that innervate the sympathetic preganglionic neurons are usually thought to be selectively responsible for the effect of this cell group on sympathetic tone and blood pressure (Reis et al., 1989; Ruggiero et al., 1994; Marina et al., 2011; Guyenet et al., 2013). Under anesthesia or in reduced preparations, this interpretation is probably correct even though the subset of C1 neurons that innervate the intermediolateral cell column also target the parabrachial nuclei, the periaqueductal gray matter and very possibly the nucleus of the solitary tract and the locus coeruleus, each of which contains neurons that impact a range of autonomic functions (Haselton and Guyenet, 1990; Card et al., 2006; Abbott et al., 2012) (Figure 5). A large portion of the C1 cells that do not innervate the spinal cord project to the hypothalamus (Tucker et al., 1987; Stornetta et al., 1999). Although the details of their connections are not known, in the aggregate, these C1 neurons innervate many hypothalamic regions that also control blood pressure and respiration such as the dorsomedial nucleus, the paraventricular nucleus and, as shown here, the orexinergic neurons (Card et al., 2006; Abbott et al., 2013b). Elsewhere in the brain, the C1 cells signal via glutamate and ionotropic glutamate receptors (Depuy et al., 2013; Guyenet et al., 2013; Holloway et al., 2013; Abbott et al., 2014), therefore the C1 projection to the orexinergic neurons also very likely has an ionotropic glutamatergic component. This interpretation is consistent with the predominantly asymmetric nature of the synapses and the fact that the terminals are filled with small clear vesicles. It is also consistent with prior evidence that, in both rats and mice, the projections of the C1 cells, including those to the hypothalamus, are largely VGLUT2-ir (Depuy et al., 2013; Abbott et al., 2013b).

The orexin neurons have a well-documented stimulatory and state-dependent effect on blood pressure and respiration. The effect of the orexin system on blood pressure is likely mediated via multiple pathways including direct projections to the intermediolateral cell column and several midbrain and lower brainstem relays, notably the RVLM (Llewellyn-Smith et al., 2003; Adamantidis and de Lecea L., 2009; Huang et al., 2010; Kuwaki and Zhang, 2010). The respiratory effects of orexin are also presumably partly mediated by projections to lower brainstem respiratory centers, including the RTN and the medullary raphe (Dias et al., 2009a; Dias et al., 2009b; Corcoran et al., 2010; Lazarenko et al., 2011). In addition, the orexinergic neurons are directly stimulated by CO_2 and contribute to the hypercapnic ventilatory reflex (Williams et al., 2007; Li et al., 2013b). The input from the C1 cells to the orexin neurons is thus one example of a long-loop pathway through which the C1 neurons that do not directly innervate the spinal cord could be regulating blood

pressure. Judging from the overall pattern of innervation of the hypothalamus by the C1 cells, additional hypothalamic loops are likely to contribute to the cardiorespiratory effects produced by the C1 cells (Card et al., 2006; Abbott et al., 2013b). The most plausible relays are the dorsomedial nucleus and the parvocellular division of the paraventricular nucleus (Dampney et al., 2008; Geerling et al., 2010). The C1-hypothalamus connection, including the projection to the orexin neurons is also likely to contribute to the arousal elicited by selective activation of the C1 cells in sleeping rats (Abbott et al., 2013a). This arousal response could also be partly mediated via direct excitatory projections of the C1 cells to other wake-promoting structures such as the locus coeruleus and the lateral parabrachial region (Card et al., 2006; Carter et al., 2010; Berridge et al., 2012; O'Donnell et al., 2012; Kaur et al., 2013; Holloway et al., 2013; Abbott et al., 2013b) (Figure 5). Finally, the orexin neurons contribute to the increase in adrenaline release from the adrenal medulla elicited by glucoprivation (Korim et al., 2014). This glucoprivic response is also triggered by stimuli that activate the C1 neurons such as hypoxia and hypotension and the increase in plasma epinephrine release elicited by administration of 2-deoxyglucose is reduced by 75% by lesions of the C1 cells (Madden et al., 2006). It is therefore probable that long-loop pathways involving the hypothalamus, especially the orexin neurons, are also implicated in the effect of the C1 cells on blood glucose. In addition, bulbospinal C1 cells are likely to mediate the peripheral release of adrenaline elicited by activation of the orexin neurons (Korim et al., 2014).

In conclusion, orexin neurons are an essential link between emotional stress and its cardiorespiratory correlates (Kuwaki, 2010). Asphyxia, hypoxia, pain and hypotension, stimuli that activate a majority of the C1 cells, likely stimulate breathing, the circulation and peripheral adrenaline release at least partly via a hypothalamic loop involving the orexin neurons. These autonomic effects of the C1 cells are presumably amplified by the concomitant arousal produced by C1 cell stimulation (Abbott et al., 2013a). Figure 5 summarizes these concepts.

Acknowledgments

This work was supported by the following grants from the National Institutes of Health (HL28785 and HL74011 to PGG).

LITERATURE CITED

Abbott SB, Coates MB, Stornetta RL, Guyenet PG. Optogenetic Stimulation of C1 and Retrotrapezoid Nucleus Neurons Causes Sleep State-Dependent Cardiorespiratory Stimulation and Arousal in Rats. Hypertension. 2013a; 61:835–841. [PubMed: 23438930]

Abbott SB, Depuy SD, Nguyen T, Coates MB, Stornetta RL, Guyenet PG. Selective optogenetic activation of rostral ventrolateral medullary catecholaminergic neurons produces cardiorespiratory stimulation in conscious mice. J Neurosci. 2013b; 33:3164–3177. [PubMed: 23407970]

Abbott SB, Holloway BB, Viar KE, Guyenet PG. Vesicular glutamate transporter 2 is required for the respiratory and parasympathetic activation produced by optogenetic stimulation of catecholaminergic neurons in the rostral ventrolateral medulla of mice in vivo. Eur J Neurosci. 2014; 39:98–106. [PubMed: 24236954]

Abbott SB, Kanbar R, Bochorishvili G, Coates MB, Stornetta RL, Guyenet PG. C1 neurons excite locus coeruleus and A5 noradrenergic neurons along with sympathetic outflow in rats. J Physiol. 2012; 590:2897–2915. [PubMed: 22526887]

Abbott SB, Stornetta RL, Fortuna MG, Depuy SD, West GH, Harris TE, Guyenet PG. Photostimulation of retrotrapezoid nucleus phox2b-expressing neurons in vivo produces long-lasting activation of breathing in rats. J Neurosci. 2009a; 29:5806–5819. [PubMed: 19420248]

Abbott SB, Stornetta RL, Socolovsky CS, West GH, Guyenet PG. Photostimulation of channelrhodopsin-2 expressing ventrolateral medullary neurons increases sympathetic nerve activity and blood pressure in rats. J Physiol. 2009b; 587:5613–5631. [PubMed: 19822543]

Adamantidis A, de Lecea L. The hypocretins as sensors for metabolism and arousal. J Physiol. 2009; 587:33–40. [PubMed: 19047201]

Adamantidis AR, Zhang F, Aravanis AM, Deisseroth K, De Lecea L. Neural substrates of awakening probed with optogenetic control of hypocretin neurons. Nature. 2007; 450:420–424. [PubMed: 17943086]

Berridge CW, Schmeichel BE, Espana RA. Noradrenergic modulation of wakefulness/arousal. Sleep Med Rev. 2012; 16:187–197. [PubMed: 22296742]

Bochorishvili G, Stornetta RL, Coates MB, Guyenet PG. Pre-Botzinger complex receives glutamatergic innervation from galaninergic and other retrotrapezoid nucleus neurons. J Comp Neurol. 2012; 520:1047–1061. [PubMed: 21935944]

Card JP, Sved JC, Craig B, Raizada M, Vazquez J, Sved AF. Efferent projections of rat rostroventrolateral medulla C1 catecholamine neurons: Implications for the central control of cardiovascular regulation. J Comp Neurol. 2006; 499:840–859. [PubMed: 17048222]

Cardin JA, Carlen M, Meletis K, Knoblich U, Zhang F, Deisseroth K, Tsai LH, Moore CI. Targeted optogenetic stimulation and recording of neurons in vivo using cell-type-specific expression of Channelrhodopsin-2. Nat Protoc. 2010; 5:247–254. [PubMed: 20134425]

Carter ME, Yizhar O, Chikahisa S, Nguyen H, Adamantidis A, Nishino S, Deisseroth K, De Lecea L. Tuning arousal with optogenetic modulation of locus coeruleus neurons. Nat Neurosci. 2010; 13:1526–1533. [PubMed: 21037585]

Corcoran A, Richerson G, Harris M. Modulation of respiratory activity by hypocretin-1 (orexin A) in situ and in vitro. Adv Exp Med Biol. 2010; 669:109–113. [PubMed: 20217331]

Dampney RA, Horiuchi J, McDowall LM. Hypothalamic mechanisms coordinating cardiorespiratory function during exercise and defensive behaviour. Auton Neurosci. 2008; 142:3–10. [PubMed: 18725186]

Depuy SD, Stornetta RL, Bochorishvili G, Deisseroth K, Witten I, Coates MB, Guyenet PG. Glutamatergic neurotransmission between the C1 neurons and the parasympathetic preganglionic neurons of the dorsal motor nucleus of the vagus. J Neurosci. 2013; 33:1486–1497. [PubMed: 23345223]

Dias MB, Li A, Nattie E. The orexin receptor 1 (OX(1)R) in the rostral medullary raphe contributes to the hypercapnic chemoreflex in wakefulness, during the active period of the diurnal cycle. Respir Physiol Neurobiol. 2009a; 170:96–102. [PubMed: 19995618]

Dias MB, Li A, Nattie EE. Antagonism of orexin receptor 1 (OX1R) in the retrotrapezoid nucleus (RTN) inhibits the ventilatory response to hypercapnia predominantly in wakefulness. J Physiol. 2009b; 587:2059–2067. [PubMed: 19273574]

Duale H, Waki H, Howorth P, Kasparov S, Teschemacher AG, Paton JF. Restraining influence of A2 neurons in chronic control of arterial pressure in spontaneously hypertensive rats. Cardiovasc Res. 2007; 76:184–193. [PubMed: 17643401]

Ericsson A, Kovacs KJ, Sawchenko PE. A functional anatomical analysis of central pathways subserving the effects of interleukin-1 on stress-related neuroendocrine neurons. J Neurosci. 1994; 14:897–913. [PubMed: 8301368]

Estabrooke IV, McCarthy MT, Ko E, Chou TC, Chemelli RM, Yanagisawa M, Saper CB, Scammell TE. Fos expression in orexin neurons varies with behavioral state. J Neurosci. 2001; 21:1656–1662. [PubMed: 11222656]

Farnham MM, Li Q, Goodchild AK, Pilowsky PM. PACAP is expressed in sympathoexcitatory bulbospinal C1 neurons of the brain stem and increases sympathetic nerve activity in vivo. Am J Physiol Regul Integr Comp Physiol. 2008; 294:R1304–R1311. [PubMed: 18272663]

Geerling JC, Shin JW, Chimenti PC, Loewy AD. Paraventricular hypothalamic nucleus: axonal projections to the brainstem. J Comp Neurol. 2010; 518:1460–1499. [PubMed: 20187136]

Guyenet PG, Stornetta RL, Bochorishvili G, Depuy SD, Burke PG, Abbott SB. Invited Review EB 2012 C1 neurons: the body's EMTs. Am J Physiol Regul Integr Comp Physiol. 201310.1152/ajpregu.00054.2013

Haselton JR, Guyenet PG. Ascending collaterals of medullary barosensitive neurons and C1 cells in rats. Am J Physiol Regul Integr Comp Physiol. 1990; 258:R1051–R1063.

Hokfelt T, Fuxe K, Goldstein M, Johansson O. Immunohistochemical evidence for the existence of adrenaline neurons in the rat brain. Brain Res. 1974; 66:235–251.

Holloway BB, Stornetta RL, Bochorishvili G, Erisir A, Viar KE, Guyenet PG. Monosynaptic glutamatergic activation of locus coeruleus and other lower brainstem noradrenergic neurons by the c1 cells in mice. J Neurosci. 2013; 33:18792–18805. [PubMed: 24285886]

Huang SC, Dai YW, Lee YH, Chiou LC, Hwang LL. Orexins depolarize rostral ventrolateral medulla neurons and increase arterial pressure and heart rate in rats mainly via orexin 2 receptors. J Pharmacol Exp Ther. 2010; 334:522–529. [PubMed: 20494957]

Hwang DY, Carlezon WA Jr, Isacson O, Kim KS. A high-efficiency synthetic promoter that drives transgene expression selectively in noradrenergic neurons. Hum Gene Ther. 2001; 12:1731–1740. [PubMed: 11560767]

Kaur S, Pedersen NP, Yokota S, Hur EE, Fuller PM, Lazarus M, Chamberlin NL, Saper CB. Glutamatergic signaling from the parabrachial nucleus plays a critical role in hypercapnic arousal. J Neurosci. 2013; 33:7627–7640. [PubMed: 23637157]

Korim WS, Bou-Farah L, McMullan S, Verberne AJ. Orexinergic activation of medullary premotor neurons modulates the adrenal sympathoexcitation to hypothalamic glucoprivation. Diabetes. 2014 Feb 18.2014 Epub ahead of print.

Kuwaki T. Orexin links emotional stress to autonomic functions. Auton Neurosci. 2010; 161:20–27. [PubMed: 20813590]

Kuwaki T, Zhang W. Orexin neurons as arousal-associated modulators of central cardiorespiratory regulation. Respir Physiol Neurobiol. 2010; 174:43–54. [PubMed: 20416404]

Kuwaki T, Zhang W, Nakamura A, Deng BS. Emotional and state-dependent modification of cardiorespiratory function: role of orexinergic neurons. Auton Neurosci. 2008; 142:11–16. [PubMed: 18440283]

Lazarenko RM, Stornetta RL, Bayliss DA, Guyenet PG. Orexin A activates retrotrapezoid neurons in mice. Respir Physiol Neurobiol. 2011; 175:283–287. [PubMed: 21145990]

Lee MG, Hassani OK, Jones BE. Discharge of identified orexin/hypocretin neurons across the sleep-waking cycle. J Neurosci. 2005; 25:6716–6720. [PubMed: 16014733]

Li A, Hindmarch CC, Nattie EE, Paton JF. Antagonism of orexin receptors significantly lowers blood pressure in spontaneously hypertensive rats. J Physiol. 2013a Jun 24.2013 Epub ahead of print.

Li AJ, Wang Q, Dinh TT, Ritter S. Simultaneous silencing of Npy and Dbh expression in hindbrain A1/C1 catecholamine cells suppresses glucoprivic feeding. J Neurosci. 2009; 29:280–287. [PubMed: 19129404]

Li N, Li A, Nattie E. Focal microdialysis of CO(2) in the perifornical-hypothalamic area increases ventilation during wakefulness but not NREM sleep. Respir Physiol Neurobiol. 2013b; 185:349–355. [PubMed: 22999917]

Llewellyn-Smith IJ, Martin CL, Marcus JN, Yanagisawa M, Minson JB, Scammell TE. Orexin-immunoreactive inputs to rat sympathetic preganglionic neurons. Neurosci Lett. 2003; 351:115–119. [PubMed: 14583395]

Madden CJ, Stocker SD, Sved AF. Attenuation of homeostatic responses to hypotension and glucoprivation after destruction of catecholaminergic rostral ventrolateral medulla (RVLM) neurons. Am J Physiol Regul Integr Comp Physiol. 2006; 291:R751–R759. [PubMed: 16627690]

Marina N, Abdala AP, Korsak A, Simms AE, Allen AM, Paton JF, Gourine AV. Control of sympathetic vasomotor tone by catecholaminergic C1 neurones of the rostral ventrolateral medulla oblongata. Cardiovasc Res. 2011; 91:703–710. [PubMed: 21543384]

Milner TA, Abate C, Reis DJ, Pickel VM. Ultrastructural localization of phenylethanolamine N-methyltransferase-like immunoreactivity in the rat locus coeruleus. Brain Res. 1989; 478:1–15. [PubMed: 2924106]

Milner TA, Morrison SF, Abate C, Reis DJ. Phenylethanolamine N-methyltransferase-containing terminals synapse directly on sympathetic preganglionic neurons in the rat. Brain Res. 1988; 448:205–222. [PubMed: 3378146]

Minson J, Llewellyn-Smith I, Neville A, Somogyi P, Chalmers J. Quantitative analysis of spinally projecting adrenaline- synthesising neurons of C1, C2 and C3 groups in rat medulla oblongata. J Auton Nerv Syst. 1990; 30:209–220. [PubMed: 2172354]

O'Donnell J, Zeppenfeld D, McConnell E, Pena S, Nedergaard M. Norepinephrine: a neuromodulator that boosts the function of multiple cell types to optimize CNS performance. Neurochem Res. 2012; 37:2496–2512. [PubMed: 22717696]

Paxinos, G.; Watson, C. The Rat Brain in Stereotaxic Coordinates. San Diego: Elsevier Academic Press; 2005.

Peyron C, Tighe DK, Van den Pol AN, De Lecea L, Heller HC, Sutcliffe JG, Kilduff TS. Neurons containing hypocretin (orexin) project to multiple neuronal systems. J Neurosci. 1998; 18:9996–10015. [PubMed: 9822755]

Reis DJ, Ruggiero DA, Morrison SF. The C1 area of the rostral ventrolateral medulla oblongata. A critical brainstem region for control of resting and reflex integration of arterial pressure. Am J Hypertens. 1989; 2:363S–374S. [PubMed: 2574588]

Ritter S, Li AJ, Wang Q, Dinh TT. Minireview: The value of looking backward: the essential role of the hindbrain in counterregulatory responses to glucose deficit. Endocrinology. 2011; 152:4019–4032. [PubMed: 21878511]

Ross CA, Armstrong DM, Ruggiero DA, Pickel VM, Joh TH, Reis DJ. Adrenaline neurons in the rostral ventrolateral medulla innervate thoracic spinal cord: a combined immunocytochemical and retrograde transport demonstration. Neurosci Lett. 1981; 25:257–262. [PubMed: 6270602]

Ruggiero DA, Cravo SL, Golanov E, Gomez R, Anwar M, Reis DJ. Adrenergic and non-adrenergic spinal projections of a cardiovascular-active pressor area of medulla oblongata: quantitative topographic analysis. Brain Res. 1994; 663:107–120. [PubMed: 7531595]

Scammell TE, Nishino S, Mignot E, Saper CB. Narcolepsy and low CSF orexin (hypocretin) concentration after a diencephalic stroke. Neurology. 2001; 56:1751–1753. [PubMed: 11425947]

Stornetta RL. Neurochemistry of bulbospinal presympathetic neurons of the medulla oblongata. J Chem Neuroanat. 2009; 38:222–230. [PubMed: 19665549]

Stornetta RL, Akey PJ, Guyenet PG. Location and electrophysiological characterization of rostral medullary adrenergic neurons that contain neuropeptide Y mRNA in rat. J Comp Neurol. 1999; 415:482–500. [PubMed: 10570457]

Stornetta RL, Sevigny CP, Guyenet PG. Vesicular glutamate transporter DNPI/VGLUT2 mRNA is present in C1 and several other groups of brainstem catecholaminergic neurons. J Comp Neurol. 2002; 444:191–206. [PubMed: 11840474]

Tucker DC, Saper CB, Ruggiero DA, Reis DJ. Organization of central adrenergic pathways: I. Relationships of ventrolateral medullary projections to the hypothalamus and spinal cord. J Comp Neurol. 1987; 259:591–603. [PubMed: 2885348]

Verberne AJM, Stornetta RL, Guyenet PG. Properties of C1 and other ventrolateral medullary neurones with hypothalamic projections in the rat. J Physiol. 1999; 517:477–494. [PubMed: 10332096]

Williams RH, Jensen LT, Verkhratsky A, Fugger L, Burdakov D. Control of hypothalamic orexin neurons by acid and CO2. Proc Natl Acad Sci USA. 2007; 104:10685–10690. [PubMed: 17563364]

Witten IB, Steinberg EE, Lee SY, Davidson TJ, Zalocusky KA, Brodsky M, Yizhar O, Cho SL, Gong S, Ramakrishnan C, Stuber GD, Tye KM, Janak PH, Deisseroth K. Recombinase-driver rat lines: tools, techniques, and optogenetic application to dopamine-mediated reinforcement. Neuron. 2011; 72:721–733. [PubMed: 22153370]

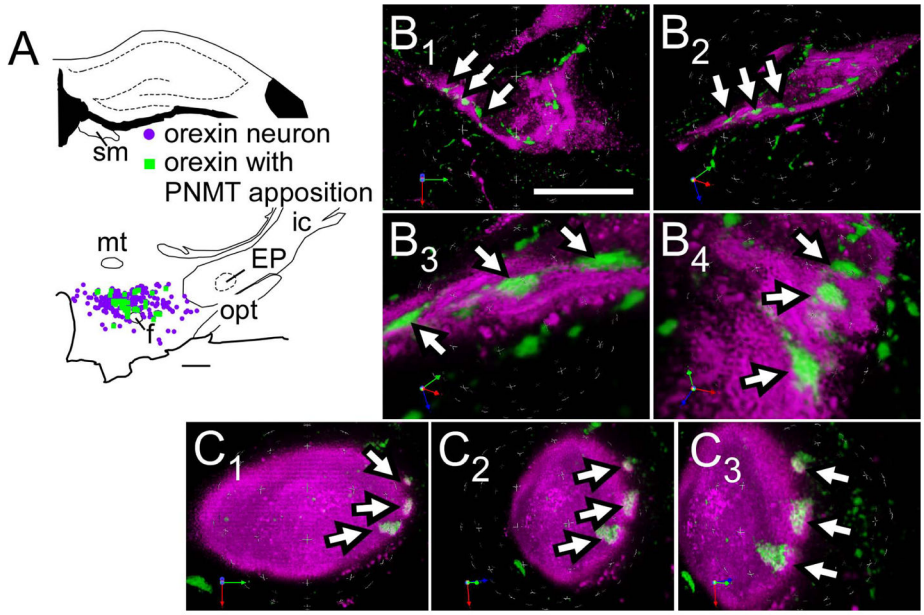

Figure 1.

Innervation of orexinergic neurons by C1 cells.

A, Computer-assisted drawing of PNMT contacts within orexin neurons.

B1–B4, C1–C3. Close appositions between PNMT terminals (revealed with Alexa-488, green fluorescence) and orexin (with Cy-3, in magenta) neurons in rats. Close appositions indicated by arrows. Putative synaptic contacts revealed through velocity 3D rendering software using deconvoluted images of 19 (in B) and 29 (in C) serial 0.3 μm Z-stacks. The overlapping region of the two fluorophores is seen as white pixels (visible in B3, B4 and C2, C3) and represents the putative contact zone.

Abbreviations: EP, entopeduncular nucleus; f, fornix; ic, internal capsule; mt, mammillothalamic tract; opt, optic tract; sm, stria medullaris of the thalamus

Scale bar A, 500 μm; B1–B2, 20 μm; B3–B4, 5 μm; C1–C3, 10 μm.

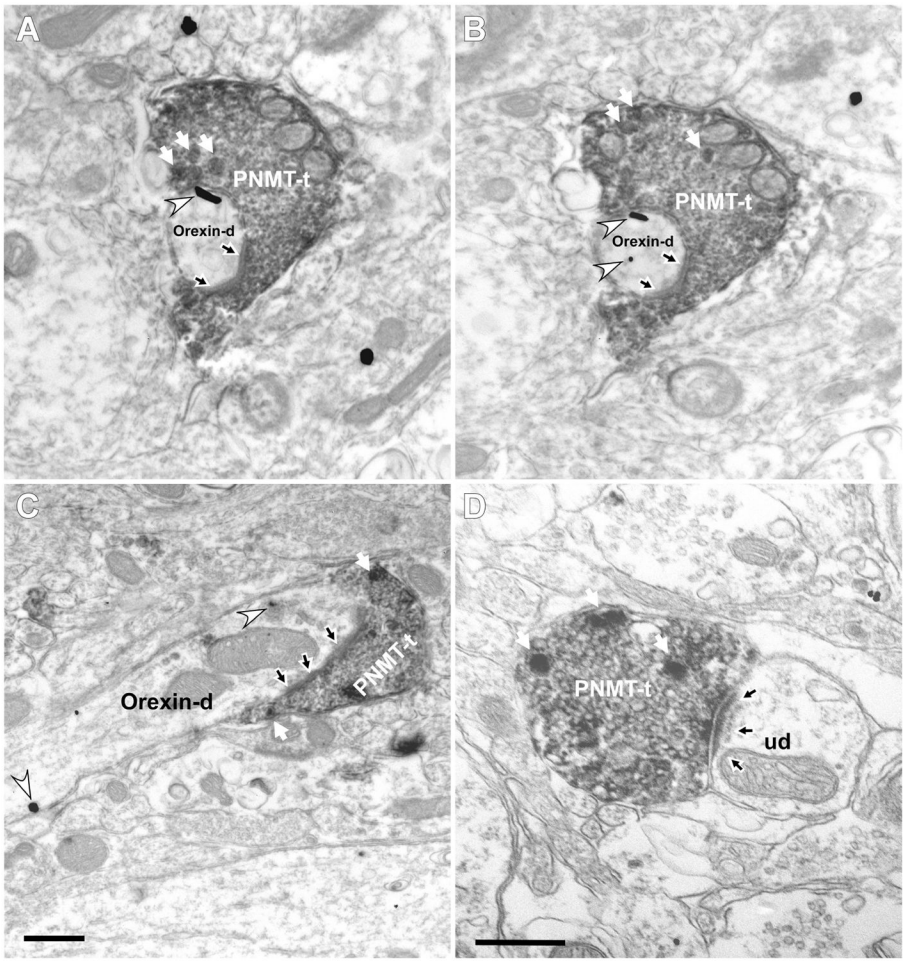

Figure 2.

PNMT-ir terminals make asymmetric synapses with both orexin-ir and other neurons in the hypothalamus. Electron micrographs show PNMT immunoperoxidase labeling (electron-dense, diffuse deposits) and orexin immunogold-silver labeling (white arrowheads). White arrows indicate dense core vesicles indicative of catecholaminergic neurons. A–C: PNMT axon terminals (PNMT-t) establish asymmetric synapses (black arrow) with orexin-immunolabeled dendrites (orexin-d). A–B; adjacent sections. D: PNMT axon terminal makes an asymmetric synapse (black arrow) on an unlabeled dendrite (ud). Scale bar 0.5 μm.

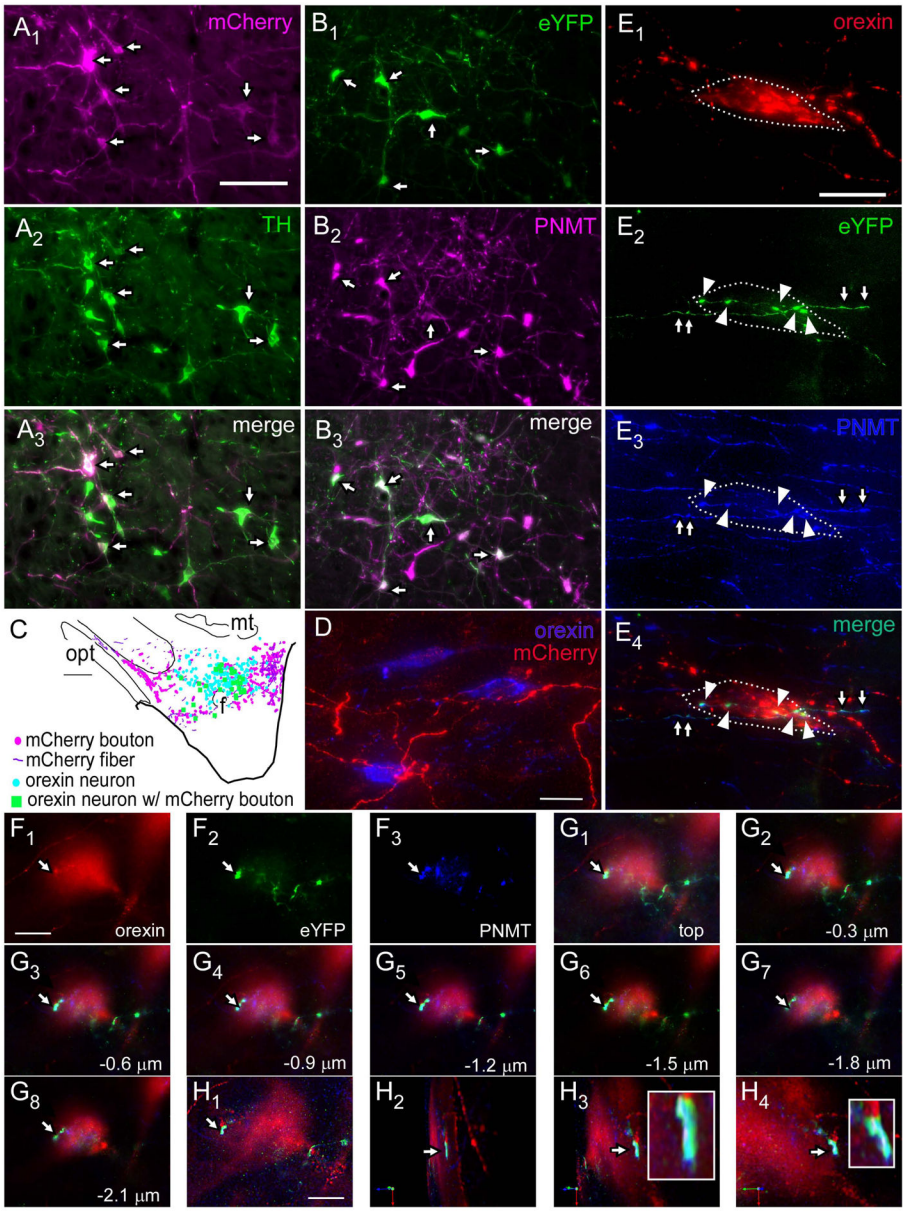

Figure 3.

C1 neurons innervate orexin neurons

A1–A3, Example of PRSX8-ChR2-mCherry lentivirus injection site in rostral ventrolateral medulla (RVLM) showing specific transduction of C1 cells, mCherry in magenta, TH in green, double-labeled cells (arrows). B1–B3, Example of injection site in RVLM from TH-Cre rat injected with Cre-dependent DIO-EF1α-eYFP-AAV2. PNMT, magenta; eYFP, green, double labeled cells (arrows). C, Computer-assisted drawings of a representative forebrain section from rat injected with PRSX8-ChR2-mCherry lentivirus in RVLM. mCherry boutons, magenta; orexin neurons without C1 close appositions, blue; orexin neurons with close appositions from C1 neurons, green. D, Close appositions in lateral hypothalamus between C1 mCherry terminals (red) from C1 cells expressing viral transgene (from lentivirus injections described in A1–A3) and orexinergic neurons; mCherry-ir fibers

and varicosities in red, orexin-ir somata, blue. E1–E4, Examples of close appositions onto an orexin cell (E1, red, outlined in white dashed line) from eYFP-ir boutons (E2, green, arrowheads) also containing PNMT, i.e. these are from C1 RVLM neurons (E3, blue), shown merged in E4. The axonal process giving rise to the boutons can also be seen outside the cell (arrows). The nerve axons and terminals in E2–E4 originated from the RVLM neurons labeled with the AAV injection described in (B1–B3). F1–F3, Another example of an orexin neuron (F1) receiving close appositions from eYFP-labeled fibers (F2) from C1 cells (i.e. PNMT-ir, F3). This neuron is shown with all color panels merged in G1. G1–G8 show serial sections of the axonal processes and boutons seen in F imaged at 0.3 μm intervals through the tissue. H1–H4. Same orexin neuron rendered in Volocity software and rotated to show close appositions (enlarged in box inset in H3–H4). Scale bars: A–B, 100 μm; in C, 500 μm; in D, 20 μm; in E, 20 μm, in F–G, 10 μm. H, 8 μm. Abbreviations: f, fornix; mt, mammillothalamic tract; opt, optic tract.

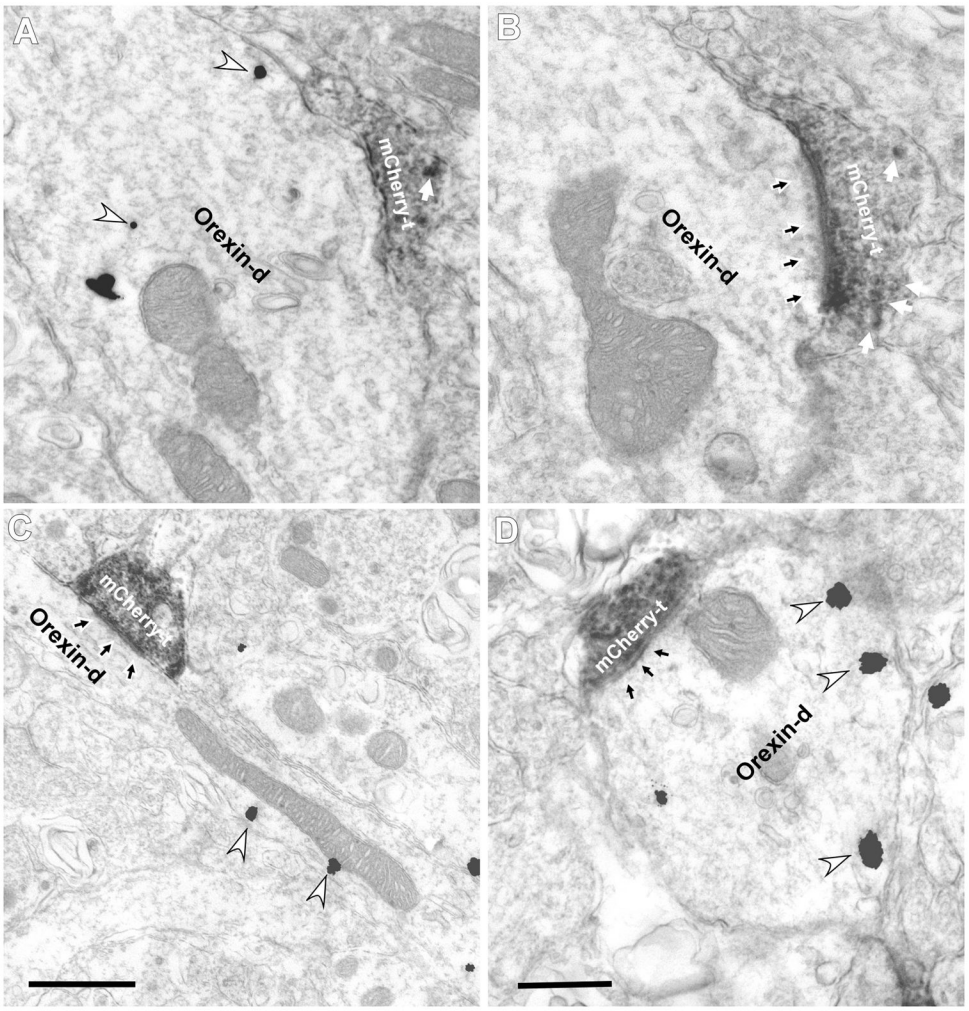

Figure 4.

mCherry axon terminals make asymmetric synapses on orexinergic neurons in the lateral hypothalamus.

Electron micrographs showing mCherry immunoperoxidase labeling (electron-dense, diffuse deposits) and orexin immunogold-silver labeling (white arrowheads). Dense core vesicles indicated by white arrows. A–B, serial sections from PRSX8-ChR2-mCherry lentivirus-injected rats showing asymmetric synapses between mCherry axon terminals (mCherry-t) and an orexin dendrite (orexin-d; black arrow). A, First serial section shows immunogold silver labeling (white arrowheads) but no synapse; in B the synapse is visible (black arrows). C, mCherry-ir axon terminal from C1 cell forms an asymmetric synapse (black arrow) with an orexin-ir dendrite in the lateral hypothalamus. D, mCherry-ir axon terminal makes a symmetric synapse with an orexin-ir dendrite. Scale bar in A–D, 0.5 μm.

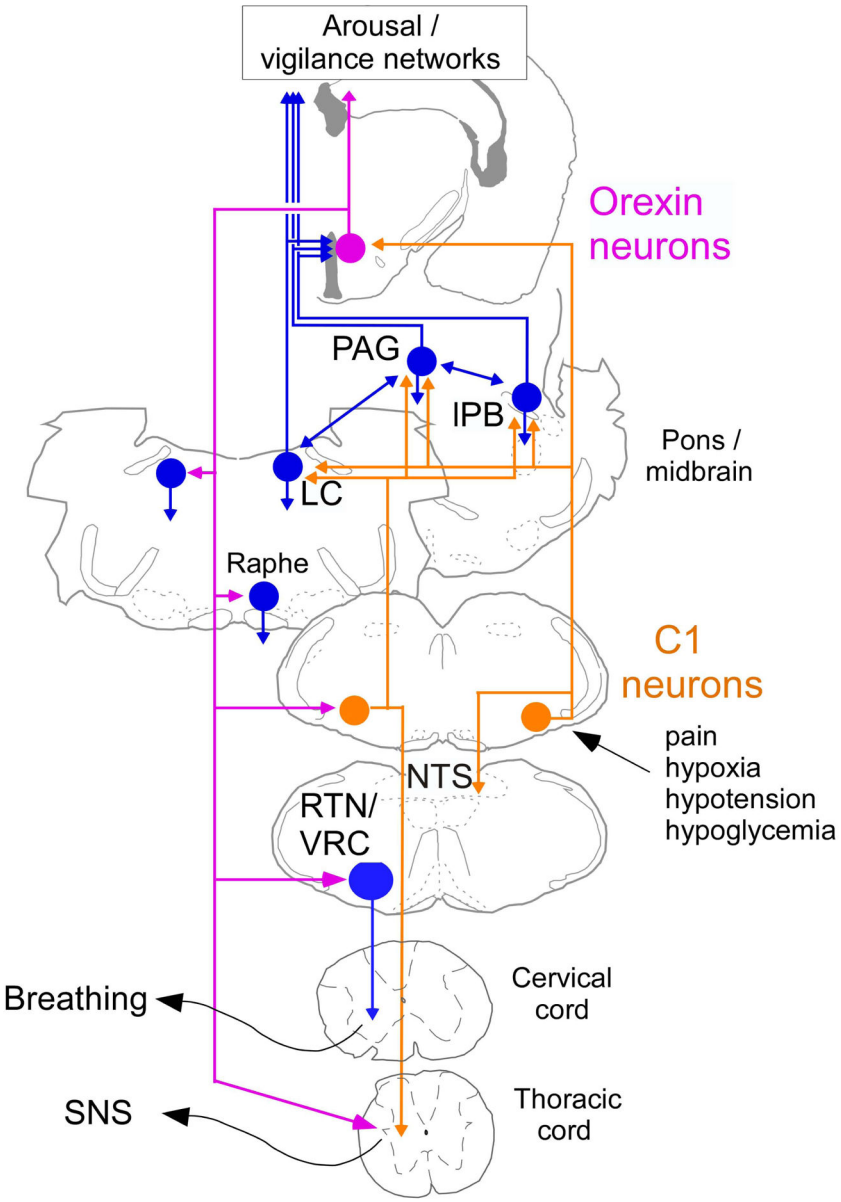

Figure 5.

Contribution of the orexin neurons to the cardiorespiratory and metabolic effects produced by activation of the C1 cells: a hypothesis.

The C1 cells are reticular formation neurons that are activated by stimuli such as pain, hypoxia, hypotension and hypoglycemia (for review (Guyenet et al., 2013)). These cells contribute to every facet of the acute stress response such as adrenaline release, increased breathing, ACTH release and cardiovascular stimulation. C1 cell stimulation also causes arousal from slow-wave sleep, an effect that is likely mediated via their projections to such wake-promoting structures as the locus coeruleus (LC), the lateral parabrachial nucleus (lPB), the periaqueductal gray matter (PAG) and, as shown here, the orexin neurons. The orexin neurons, in turn, enhance the level of vigilance and its autonomic and respiratory

correlates via their projections back to the LC, the raphe and the ventrolateral medulla. A likely target of orexin neurons are the C1 cells that innervate the sympathetic preganglionic neurons and control the sympathetic nervous system (SNS). Note that the C1 cells with projections to the hypothalamus are most likely a different population than those that project to the spinal cord, however, both of these C1 cell groups may give rise to collaterals projecting to overlapping regions of the medulla/pons.

Table 1

Antibodies

Antibody	Host, isotype	Immunogen	Source	Cat. No., Lot No., RRID	Concentration
orexin	Goat IgG	Synthetic peptide residues 48–66 of human orexin A precursor	Santa Cruz	SC-8070, C-19 C3110 RRID:AB_2315772	40 ng/ml
dsRed	Rabbit IgG	Ds-Red Express variant of *Dicosoma* sp. red fluorescent protein	Clontech	632496 1306037 RRID:AB_10015246	1 μg/ml
PNMT	Rabbit serum	Rat adrenal extract	Martha Bohn, Northwestern Univ.	PNMT (phenylethanolamine N-methyl transferase) RRID:AB_2315181	rabbit serum used at 1:10,000
TH	Sheep IgG	native TH from rat pheochromocytoma	Millipore	AB1542 1994656 RRID:AB_90755	50 ng/ml
GFP	Chicken, IgY	recombinant GFP	Aves Labs	GFP-1020 0511FP12 RRID:AB_1000024	10 μg/ml

J Comp Neurol. Author manuscript; available in PMC 2015 December 01.